Attaching SiO$_2$ nanoparticles to GO sheets via amino-terminated hyperbranched polymer for epoxy composites: Extraordinary improvement in thermal and mechanical properties

Lichun Ma [a,c,*], Guojun Song [a], XieChen Zhang [a], Shaofeng Zhou [b], Yaqing Liu [b,*], Luyan Zhang [c]

[a] Institute of Polymer Materials, College of Materials Science and Engineering, Qingdao University, Qingdao 266071, China
[b] Shanxi Province Key Laboratory of Functional Nanocomposites, North University of China, Taiyuan 030000, China
[c] School of Environmental Science and Engineering, Yancheng Institute of Technology, Yancheng 224051, China

ABSTRACT

The deposition of nano-silica (SiO$_2$) on graphene oxide (GO) surface via amino-terminated hyperbranched polymer (HBP) was designed to improve the dispersion and interfacial interaction between GO and epoxy resin. The structures and morphologies of GO and GO-SiO$_2$ sheets were characterized by FT-IR, XRD, XPS, TG, SEM and TEM. Epoxy composites containing GO and GO-SiO$_2$ with 0.1 wt% loadings were prepared and systemically investigated. It was indicated that the GO-SiO$_2$/epoxy composites displayed higher mechanical and thermal properties than that of GO or SiO$_2$ composites. For epoxy composites containing 0.1 wt% GO-SiO$_2$, the flexural strength increased by 20.57% and 23.58% compared to that of individual GO composites and individual SiO$_2$ composites, respectively. Furthermore, the reinforcing mechanisms have been also illuminated. This work is expected to be beneficial to the designing of adhesive-bonded composite structures or components.

1. Introduction

As a widely used thermosetting resin, epoxy resin has many outstanding properties such as good corrosion resistance, excellent thermal stability and eminent weather resistance, which have been widely used in coatings in electronic and aerospace industries [1–3]. However, the supernal crosslinking density of epoxy results in inherent brittleness and poor crack resistance, which restricts its application in some high performance fields [4]. Accordingly, enhancing fracture toughness of epoxy resin is indispensable. Moreover, the epoxy resins with high thermal resistance are necessary in high temperature applications. In current, many researchers have been dedicated to add nanomaterials such as graphene, carbon nanotubes, inorganic nanoparticles, etc. into epoxy resins to improve the mechanical and thermal properties [5,6].

Graphene, possessing excellent mechanical properties[7], has become an ideal candidate for assembling high performance graphene-based nanocomposites.[8–10]. However, the poor dispersion and agglomeration of graphene resulted in limited improvement in the composites mechanical and thermal properties[11,12]. To address the issues, many researchers have functionalized graphene and graphene

oxide (GO) with small molecules or polymers to achieve better dispersion and compatibility in matrix and has been verified to be an effective way[13–15]. Sahu et al. [16] have revealed that mechanical performances of GO-PAA/epoxy composites significantly improved, which was attributed to the improved dispersibility of GO-PAA and the better adhesion with the matrix. Liu et al.[17] have grafted poly (oxyalkylene) amines (D400 and D2000) onto GO sheets and noticed that the mechanical properties and thermal properties improved distinctly. Meanwhile, the tensile strength of 0.1 wt% D400-GO/epoxy and D2000-GO/epoxy composites increased by 23.5% and 21.6%, respectively.

Moreover, GO has become a carrier for adhering nanoparticles due to its high specific surface area and abundant functional groups. The nanoparticle functionalized GO could increase the interlayer spacing between GO sheets, which could exhibit a special structure and have advantageous for preventing re-stacking among GO sheets[18]. Silica nanoparticles (SiO$_2$) have received extensive attention for reinforcing epoxy resin due to low cost, high strength, high temperature resistance and chemical stability. Therefore, to make the most of GO and SiO$_2$, it is necessary to adhere SiO$_2$ to GO surface to get better dispersibility in epoxy matrix. We have attached SiO$_2$ onto GO surface through thiol-ene click chemistry reaction or diethylenetriamine (DETA) and tetraethyl

* Corresponding authors at: Institute of Polymer Materials, College of Materials Science and Engineering, Qingdao University, Qingdao 266071, China (L. Ma).
E-mail address: malc_hit@126.com (L. Ma).

orthosilicate (TEOS)[19,20]. However, some functional groups on GO were eliminated due to the coverage of SiO$_2$ onto the GO surface and no more reactive groups on SiO$_2$, which led to weak interact with epoxy matrix. Therefore, it is necessary to develop enough reactive groups on SiO$_2$ to improve the interaction between GO and epoxy matrix.

Hyperbranched polymer (HBP), has attracted more and more attention because of its three-dimensional branched structure, a large number of terminal functional groups and strong chemical reactivity [21–23]. It is expected that the HBP attached on SiO$_2$ would form a covalent bond with the hybrid material and the epoxy resin, thereby achieving better interfacial interaction. However, there have been few reports on the attachment of SiO$_2$ onto GO surface via hyperbranched polymer.

Herein, a new method to uniformly bond SiO$_2$ to the GO surface was developed. At first, the SiO$_2$ surface was modified with KH-550 and amino-terminated HBP by two Michael addition reactions. Then, the SiO$_2$-HBP was uniformly adhered on the GO surface by covalent bond. The HBP on the SiO$_2$ surface not only reacted better with the groups on GO surface, but also participated in the curing reaction of epoxy resin, which could enhance the interfacial interaction between GO and epoxy matrix effectively. Moreover, the SiO$_2$-HBP would form rigid-flexible structure on GO surface to transfer load effectively. The dispersibility, mechanical and thermal properties of GO-SiO$_2$ in epoxy resin was studied. Moreover, the enhancement principle and interaction mechanism of nanocomposites were discussed.

2. Experimental

2.1. Preparation of GO-SiO$_2$ hybrids

GO was prepared from graphite based on modified Hummers' method in our previous study[24]. The GO-SiO$_2$ hybrids were prepared by amidation reaction between carboxyl groups on the GO surface and amino-terminated hyperbranched polymer functionalized SiO$_2$. In a typical synthesis, 0.1 g GO and 0.1 g SiO$_2$-HBP were added into 100 mL N, N-dimethylformamide (DMF) and ultrasonicated for 1 h. Then, 2-(7-Azabenzotriazol-1-yl)-N,N,N',N'-tetramethyluronium hexafluor ophosphate (HATU) was mixed in the dispersion and refluxed at 80 ℃ for 4 h. Finally, the product was washed using DMF for five times and dried at 80 ℃ for 12 h, which obtained GO-SiO$_2$ hybrids. The manu-facture procedure of GO-SiO$_2$ hybrids were shown in Fig. 1.

2.2. Preparation of epoxy composites

The fabrication process GO-SiO$_2$ reinforced epoxy composites were as follows: GO-SiO$_2$ hybrids were firstly dissolved in acetone using ultrasonication for 1 h. Epoxy resins were added into the mixture with ultrasonic to ensure uniform distribution of GO-SiO$_2$. Then the mixture was also evaporated off to get rid of acetone. Subsequently, the mixture was blended with a stoichiometric amount of H-256 (2:1 w/w) with high speed stirring. In order to remove excess bubbles, the mixture was degassed in vacuum oven for 1 h. Finally, the mixture was cast into the mold and cured 2 h at 100 ℃ and 4 h at 150 ℃. For comparison, the neat epoxy, GO/epoxy, SiO$_2$/epoxy composites were fabricated with the same procedure.

2.3. Characterizations and measurements

The functional groups of GO power and its derivatives were measured by Fourier transform infrared spectroscopy (FT-IR, NEXUS). The spectral was recorded in the range from 500 cm^{-1} to 4000 cm^{-1} with the wavenumber at 4 cm^{-1} resolution. The elements chemical compositions and the functional groups were investigated by X-ray photoelectron spectroscopy (XPS, ESCALAB 220i-XL). X-ray diffraction (XRD, DX-2700) was used to confirm the internal structure. The sample was measured under the ranged from 5° to 45° with scan speed of 3°·min^{-1}. The surface microstructure of GO-SiO$_2$ hybrids and fracture surface morphology of composites were observed by Scanning electron microscopy (SEM, JSM-7800F). Before the observation, the sample need to be sprayed with gold to obtain conductivity. Transmission electron microscopy (TEM, G2F30) and optical microscopy (OM) were carried out to investigate the dispersion in epoxy matrix. The thermal stability of GO-SiO$_2$ hybrids were measured by Thermo-gravimetric analysis (TGA, DTG60H), the samples were heated from 30℃ to 800℃ with a heating rate of 10°·min^{-1} under N$_2$ atmosphere. According to GB/T2567-2008, the tensile and flexural properties of composites were tested by universal tensile machine (Al-7000) using dumbbell shaped specimens at room temperature. The impact properties of composites were conducted by impact testing machine (XJJ-50), the size of samples were 80 mm (long) × 10 mm (wide) × 4 mm (thick) and there was no gap in the sample. Each test was gathered at least five valid samples and recorded the average parameters. Dynamical Mechanical Analysis (DMA) curves were recorded on a TRITEC 2000B device. The sample was heated in a temperature range of 25–180 ℃, with a heating rate of 5 ℃/min and 1 Hz frequency. TGA-DTG analysis of composites were carried out by
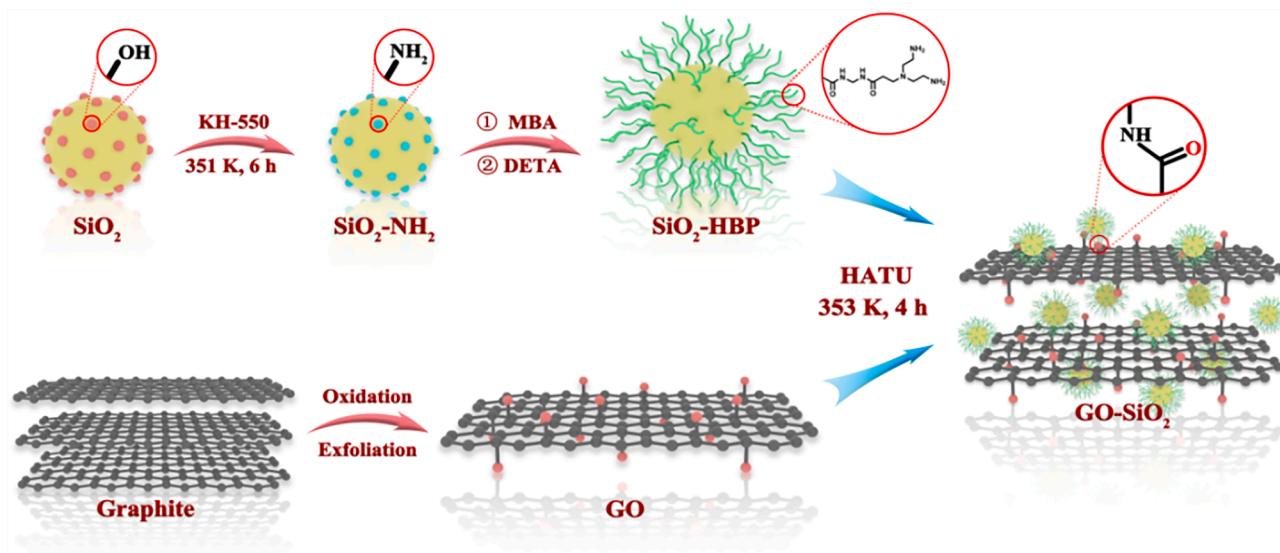

Fig. 1. Schematic illustration for the preparation of GO-SiO$_2$ hybrids.

STAR SW at temperature region of 25–700 °C and heating rate of 5 °C/min in air atmosphere.

3. Results and discussion

3.1. Characterization of GO-SiO₂ hybrids

The XPS spectra were used to further confirm the chemical composition of GO and its derivatives, as presented in Fig. 2 and Table 1S. Two peaks for GO were observed, which were carbon element (69.9%) and oxygen element (30.1%). For SiO$_2$-NH$_2$, the C1s and N1s appeared which proved successful functionalization with KH-550 onto SiO$_2$. After functionalized with HBP, the peak intensity of carbon and nitrogen gradually increased. For GO-SiO$_2$, the Si2p and N1s were observed, which implied that silica was successfully covalent bonded onto the GO surface.

The high-resolution spectra of C1s and N1s were listed in Fig. 2b-e. In Fig. 2b, GO presented five functional groups, C = C (284.4 eV), C-C (285.2 eV), C-O (286.6 eV), C = O (288.0 eV) and O-C = O (289.2 eV), which derived from the aromatic ring and the oxygen functional groups on the GO surface, respectively[25]. In Fig. 2c, owing to the introduced amine modified SiO$_2$, two new peaks were founded at 285.8 eV and 288.8 eV, which corresponded to C-N and N-C = O, respectively. Moreover, a new peak arised at 284.4 eV corresponded to C-Si, which confirmed that SiO$_2$ was chemically adhered onto GO surface successfully. The N1s band of SiO$_2$-HBP in Fig. 2d were deconvoluted to two peaks at 399.6 eV and 401.5 eV, which corresponded to –NH and N-C = O. For GO-SiO$_2$, the intensities of N1s band at 401.5 eV distribution to N-C = O increased, which implied that the amidation reaction occurred between GO and SiO$_2$. These consequences also afforded the testimony for the successful attachment of SiO$_2$ onto the GO surface via covalent bond.

The TGA and DTG results showed the weight loss of SiO$_2$, SiO$_2$-NH$_2$, SiO$_2$-HBP, GO and GO-SiO$_2$ hybrids under N$_2$ atmosphere (Fig. 3). SiO$_2$ presented good thermal stability which came to the char residue of 93.63% at 800 °C. SiO$_2$-NH$_2$ displayed two mass loss stages, the first weight lost were founded in the range of 30–100 °C, which was attributed to evaporation of water on the surface of SiO$_2$-NH$_2$. The second weight lost occurred at 500°C was probably owing to the decomposition of amine groups and carbon chain of silane molecules[26]. Compared to SiO$_2$-NH$_2$, the char residue of SiO$_2$-HBP declined by 6.20% from 90.90% to 84.70%. The decrease in char residue was mainly due to the decomposition of hyperbranched polymer, indicating that the nano-SiO$_2$ was successfully modified by hyperbranched polymer. In the case of GO, there were three temperature intervals of mass loss: (1) Weight loss from 30 °C to 140 °C was because of the volatilization of absorbed water; (2) The weight loss in the temperature range of 140-330°C was caused from the decomposition of the oxygen-containing functional groups on the GO surface; (3) The weight loss over 330 °C was attributed to the decomposition of carbon skeleton[27]. The decomposition behavior of GO-SiO$_2$ hybrids was similar to GO. However, compared with GO, the thermal stability of GO-SiO$_2$ hybrids improved greatly. In addition, the decomposition rate of GO-SiO$_2$ hybrids was significantly slower than GO from the DTG curve, which was mainly due to the deposition of hyperbranched polymer grafted SiO$_2$ onto GO surface. Therefore, adhering SiO$_2$ was advantageous to improve the GO thermal stability.

3.2. Morphology of GO-SiO₂ hybrids

The morphologies and structures of GO and GO-SiO$_2$ hybrids were investigated by SEM and TEM. Fig. 4a showed that GO has a sheet-like structure with many wrinkles [28]. Compared with GO, the GO surface was uniformly covered with a layer of nano-silica in Fig. 4b, and became extremely rough. The TEM image of GO and GO-SiO$_2$ hybrids (Fig. 4c-d) were further used to analyze the morphological structure. The GO surface was glazed and tidy and there were some small ripples on GO surface. This was consistent with the SEM results. The TEM image of GO-SiO$_2$ hybrids showed that a large amount of nano-SiO$_2$ has adhered uniformly to the GO surface. This further proved that GO-SiO$_2$ hybrids were successful synthesized. Moreover, the wrinkled GO
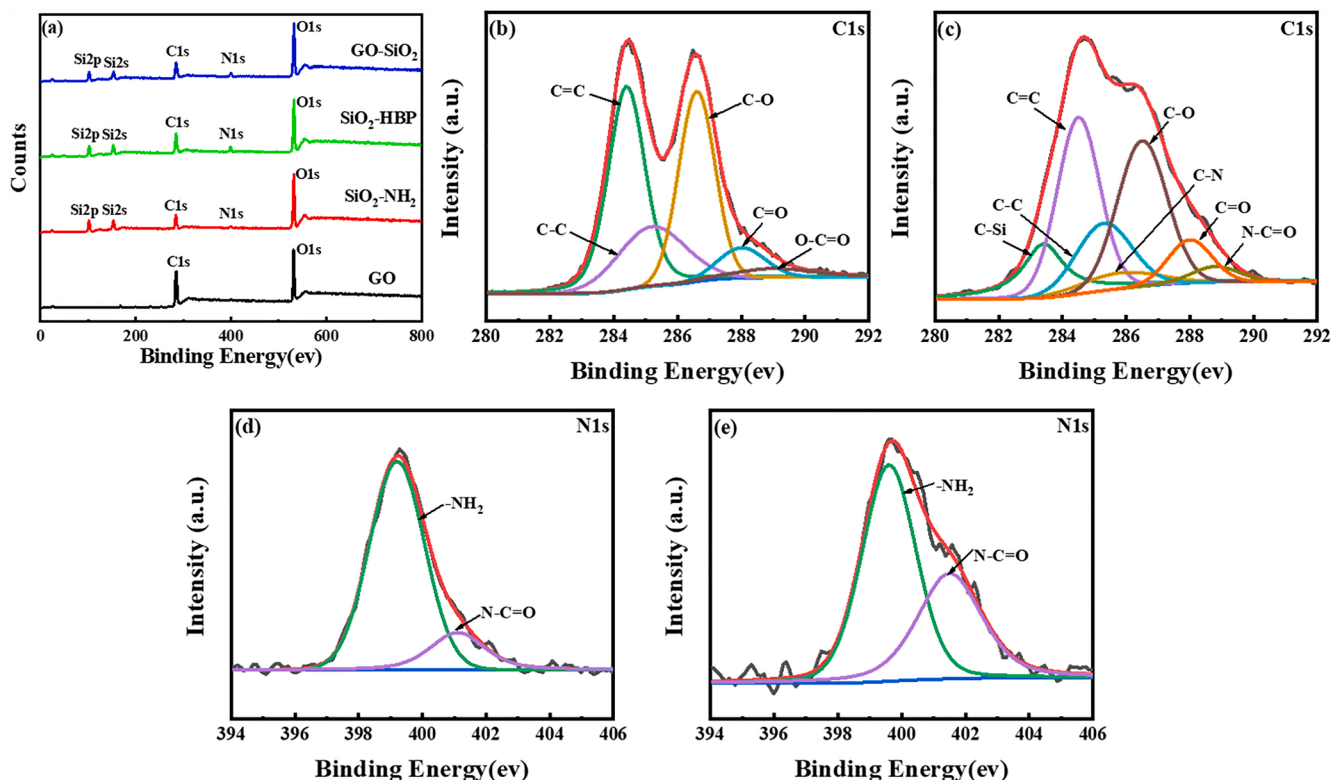

Fig. 2. (a) XPS spectra, (b) C1s spectra of GO and (c) GO-SiO₂, (d) N1s spectra for SiO₂-HBP and (f) GO-SiO₂
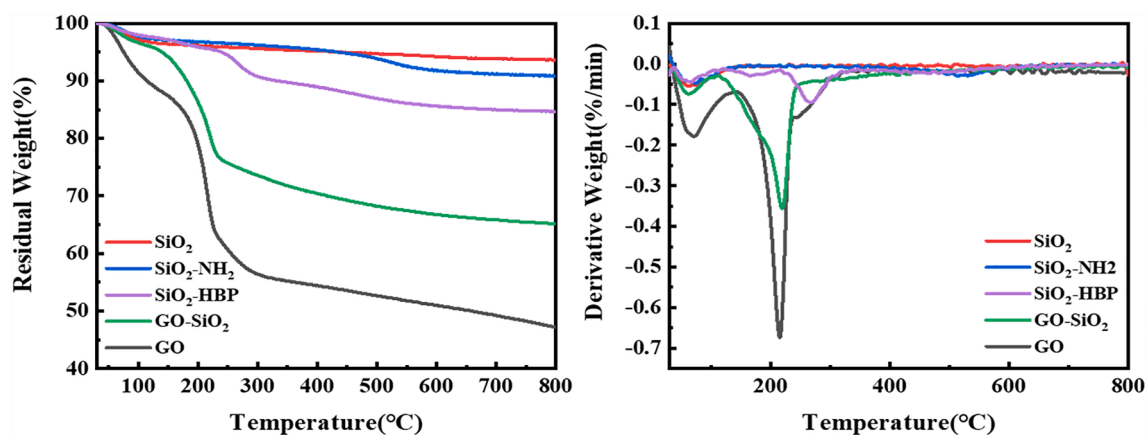
Fig. 3. TGA (a) and DTG (b) curves of SiO$_2$, SiO$_2$-NH$_2$, SiO$_2$-HBP, GO, GO-SiO$_2$.
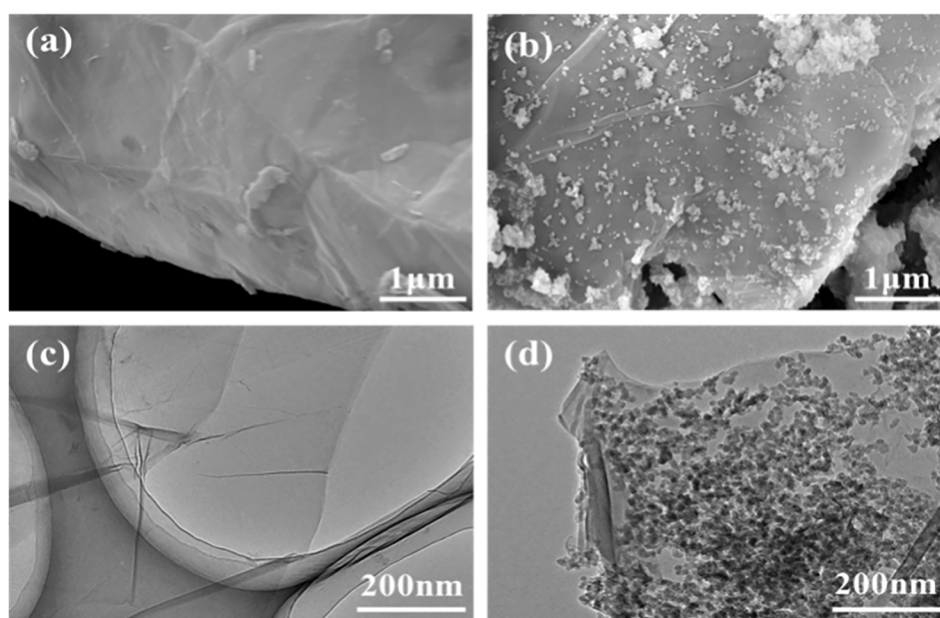

Fig. 4. SEM and TEM images of GO (a, c) and GO-SiO$_2$ (b, d).

nanolayers with coverage of hyperbranched polymer grafted SiO$_2$ particles would offer strong interfacial interaction with polar polymer matrix [29].

OM and TEM measurements were performed to investigate the dispersibility and interfacial compatibility of GO and GO-SiO$_2$ hybrids in epoxy resin, as shown in Fig. 5. In Fig. 5a, GO (0.1 wt%) was easy to aggregate and presented poor dispersion in epoxy matrix due to its large specific surface area and van der Waals force[30]. TEM results showed similar situation in Fig. 5c. In contrast, it could be seen in Fig. 5b that the aggregates were significantly less than GO, which indicated that SiO$_2$ could inhibit the re-aggregation of GO and thereby improved dispersion in matrix. Moreover, the GO-SiO$_2$ hybrid emerged better embedding in the epoxy matrix in Fig. 5d compared with that of GO because that the SiO$_2$ surface was grafted with amino-terminated hyperbranched polymer. It was also anticipated that better dispersion and interfacial interaction of GO-SiO$_2$ hybrids would be conducive to improve thermal and mechanical properties in composites.

The thermo-mechanical properties of GO, SiO$_2$ and GO-SiO$_2$ reinforced epoxy nanocomposites were investigated by DMA. The curves of storage modulus, loss modulus and loss factor (tan δ) of the neat epoxy and nanocomposites were presented in Fig. 6a, b, c. The value of storage modulus and glass transition temperature (T_g) of the nanocomposites

were listed in Table 2S. The storage modulus declined as the temperature increased owing to the softening of polymer matrix[31]. The storage modulus of GO-SiO$_2$/epoxy (19.2 MPa at 125 °C) was higher than that of epoxy, GO/epoxy and SiO$_2$/epoxy nanocomposites, which was mainly benefited from the well dispersion and an improved interfacial interaction between GO-SiO$_2$ sheets and epoxy, confirmed by the OM and TEM measurements. Moreover, the SiO$_2$-NH$_2$ grafted onto the GO surface could react with the epoxy resin. Thus, the introduction of GO-SiO$_2$ was supposed to improve the storage modulus of the GO/epoxy nanocomposites.

T_g was calculated on the basis of the temperature at maximum loss modulus, the GO-SiO$_2$/epoxy presented the highest T_g, a good dispersity and strong interfacial interactions between the GO-SiO$_2$ and epoxy matrix promoted heat and stress transfer, which was a important factor for the performance enhancement of the GO-SiO$_2$/epoxy nanocomposites. The GO-SiO$_2$ could also boost the curing rate and cross-linking density of the epoxy due to the reactions between the amino groups and the epoxy groups[32].

The thermal stability of nanocomposites reinforced with GO, SiO$_2$ and GO-SiO$_2$ was measured in air and a two-stage degradation was presented in Fig. 6c, the first range up to 400 °C ascribed to labile bond cleavage and the second stage up to 600 °C assigned to char formation
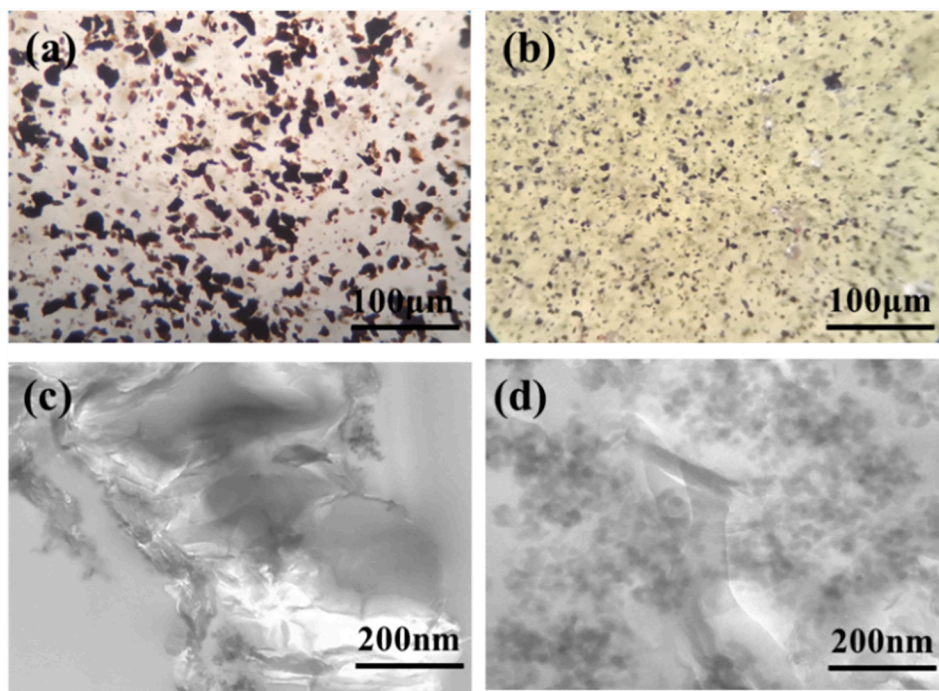
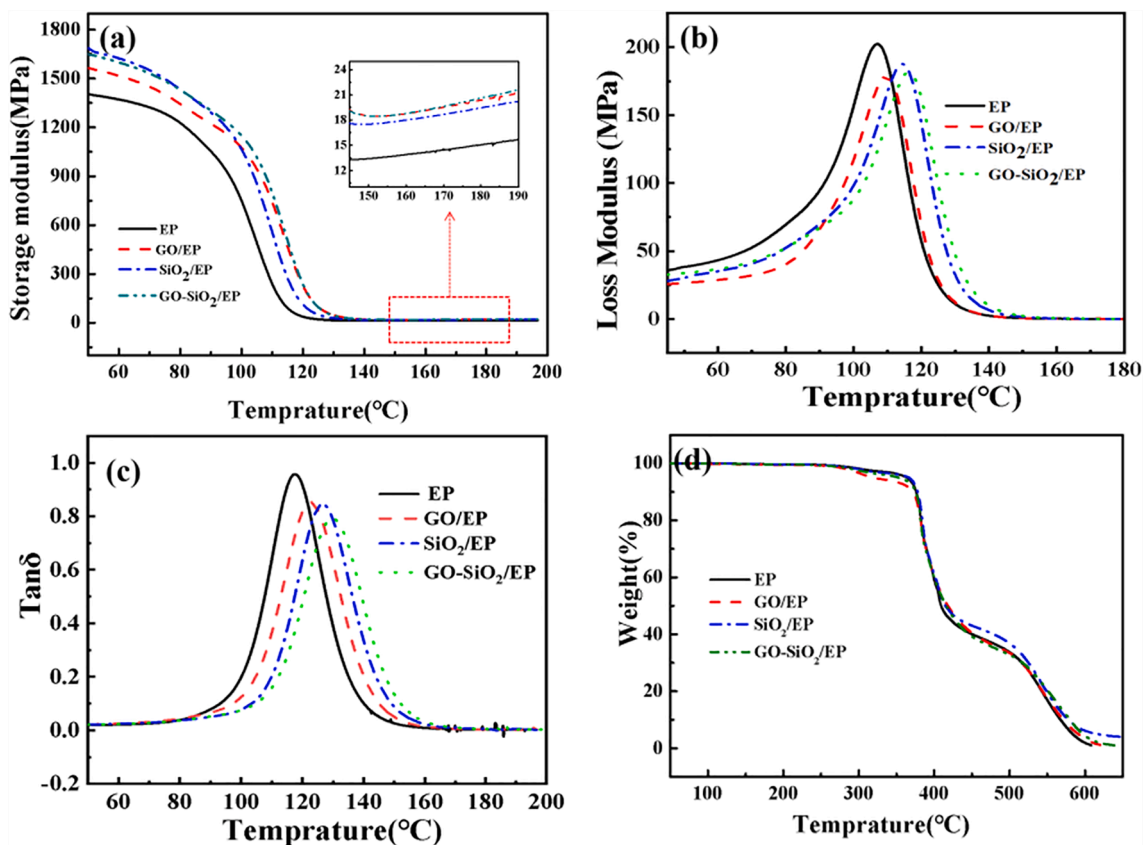**Fig. 5.** OM and TEM images of nanocomposites: (a, c) 0.1 wt% of GO/EP, (b, d) 0.1 wt% of GO-SiO$_2$/EP.

Fig. 6. Storage modulus (a), loss factor (tanδ) (b) and loss modulus (c) from DMA and TGA curves (d) for epoxy and its nanocomposites.

and graphitization[33]. The decomposition temperature (T_d) for pure epoxy and GO/epoxy was near 530 ℃. However, the T_d of SiO$_2$-GO/ epoxy reached 578 ℃, which strongly implied the increment of thermal stability of epoxy by introducing SiO$_2$-GO nanohybrid. The better

thermal stability of SiO$_2$-GO/epoxy might be attributed to stabilizing mechanism against heat penetration, the SiO$_2$-GO nanohybrids could act as a barrier against heat and postpone it[34].

3.3. Mechanical properties of composites

Fig. 7 and Table 3S showed the tensile and flexural performances of pure epoxy and its composite with 0.1 wt% filler. The tensile strength and elastic modulus of pure resin were 64.5 ± 2.8 MPa and 2.6 ± 0.1 GPa, respectively. The tensile strength and modulus of GO/EP and SiO$_2$/EP increased by 20.28%, 19.32% and 17.61%, 7.20% compared with pure epoxy, respectively, which indicated that nano-particle had obvious enhancement effect, even with a small amount of addition in epoxy resin. Surprisingly, the composites reinforced with 0.1 wt% GO-SiO$_2$ showed 37.81% and 28.41% improvements in tensile strength and elastic modulus (88.8 ± 4.3 MPa, 3.4 ± 0.2 GPa) compared with pure epoxy, respectively. Moreover, the flexural strength and modulus of GO-SiO$_2$ composites enhanced by 20.57%, 2.15% and 23.58%, 9.21% compared with that of GO and SiO$_2$ composites. This manifested that the reinforcement effect of GO-SiO$_2$ hybrids on epoxy composites was more effective than individual GO or SiO$_2$. It is expected that the adhering of HBP grafted SiO$_2$ particles onto GO sheets could generate a particular

three-dimensional point-plane structure and play a synergistic effect, furthermore, the polar-polar interaction between HBP and epoxy resin could increase the interfacial adhesion, so that the stress can be transferred and dispersed from matrix to GO-SiO$_2$ effectively and increased the mechanical performances.

The impact strength of pure epoxy and its composites with GO, SiO$_2$ and GO-SiO$_2$ was presented in Fig. 7e. The composites with 0.1 wt% GO and SiO$_2$ showed about 23.83% and 30.91% improvement compared to the pure epoxy, which was on account of the strong interfacial interaction between the oxygen functionalities of GO or SiO$_2$ and the epoxide groups of resin[35,36]. Surprisingly, the composites reinforced with 0.1 wt% GO-SiO$_2$ showed 86.86% improvements in impact strength (39.5 ± 3.0 kJ/m^2), which was ascribed to the high aspect ratio of GO-SiO$_2$, better dispersion and interfacial interaction of GO-SiO$_2$ with epoxy. Therefore, the adhering of SiO$_2$-HBP onto GO sheets might be conducive to consume more fracture energy and facilitate the stress transfer and lead to an enhancement in impact strength.

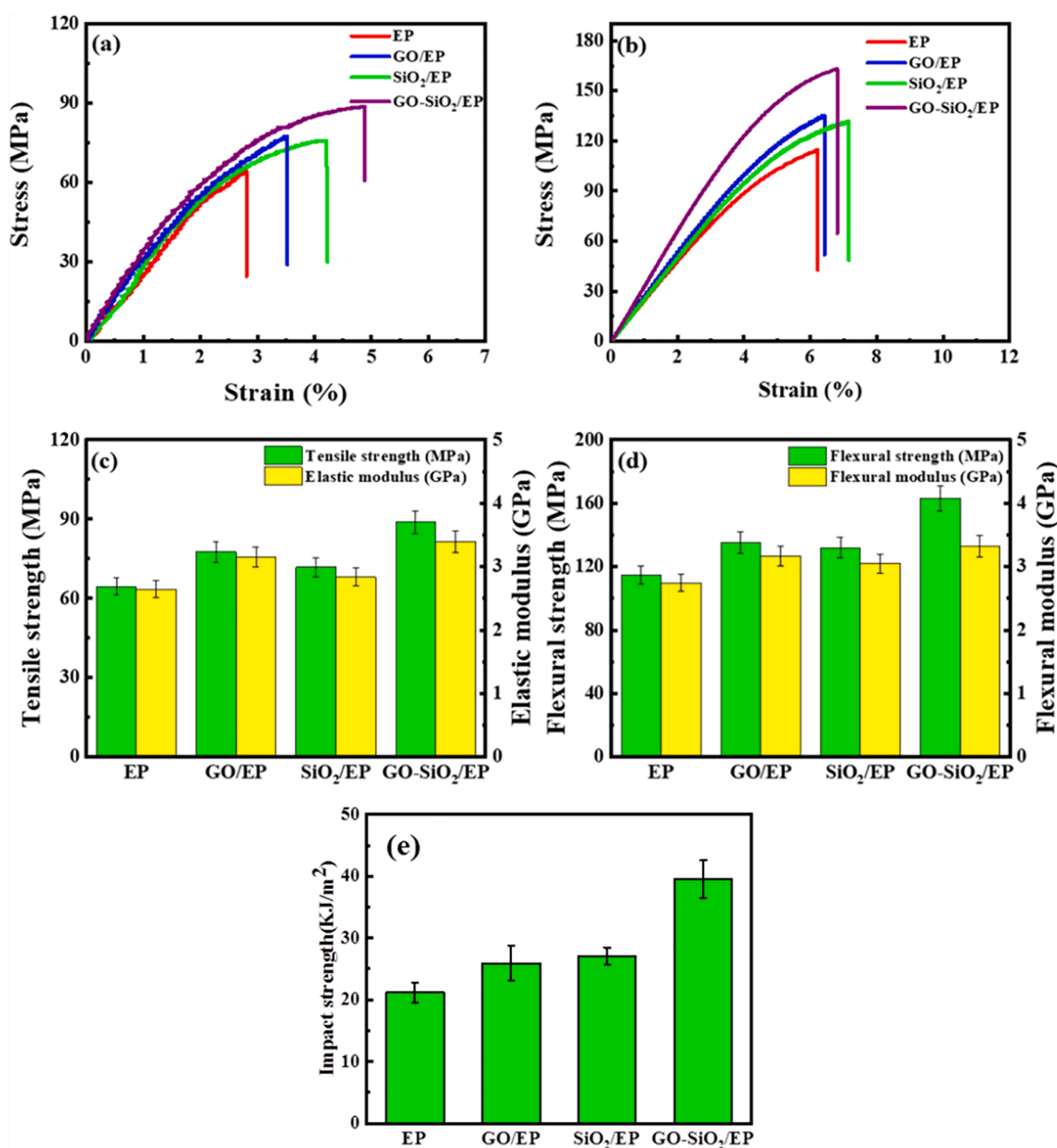In order to understand the enhancement mechanism of composites,

Fig. 7. Mechanical properties of epoxy and its nanocomposites: (a) stress–strain curves of tensile; (b) stress–strain curves of flexural; (c) tensile strength and elastic modulus; (d) flexural strength and modulus; (e) impact strength.

the fracture surfaces morphologies of GO/EP and GO-SiO$_2$/EP composites after impact were observed by SEM, as shown in Fig. 8. For GO/EP (Fig. 8a), there were some ripples and obvious gaps on the surface, manifesting unevenly dispersed and weak interfacial adhesion between GO and epoxy resin. Relatively, the surface of GO-SiO$_2$/EP emerged step-like delamination and numerous smaller ripples in Fig. 8b, and some GO-SiO$_2$ sheets appeared to well disperse in the epoxy. The generation of the ripples was accompanied by the creation of new fracture surfaces [37], and much more fracture energy would be expended for GO-SiO$_2$/epoxy composites.

The improved mechanical performances of composites at lower filler loadings might be ascribed to the following mechanisms: (1) The attachment of SiO$_2$ on GO surface might suppress re-aggregation to improve dispersibility in epoxy matrix; (2) The grafting of amino-terminated hyperbranched polymer onto SiO$_2$ surface might facilitate the formation of covalent bonds and interlocking effect with epoxy resin, thereby enhancing the interfacial adhesion of GO-SiO$_2$ with the resin [38]; (3) The peculiar three-dimensional point-plane structure of GO-SiO$_2$-HBP might conduce to produce a gradient modulus interface with the epoxy to transfer load effectively; (4) More fracture energy was absorbed effectively by SiO$_2$-HBP rigid-flexible structure, meanwhile, the propagation path of crack became more complicated and tortuous, the schematic diagram of stress transfer in nanocomposites was exhibited in Fig. 10a,b. Therefore, HBP, SiO$_2$ and GO could exert the synergistic strengthening and toughening effect, and increase the mechanical properties of composite.

4. Conclusion

In this work, a new strategy for preparing GO-SiO$_2$ hybrids with the assistance of amino-terminated hyperbranched polymer has been developed and incorporated epoxy to obtain superior mechanical and thermal properties of composites. The silica functionalized by amino-terminated hyperbranched polymer could be easily adhered to the GO surface through covalent bonds, improving the dispersibility of GO and promoting better interaction with epoxy matrix. The storage modulus, tensile, flexural, impact strength and storage modulus for 0.1 wt% GO-SiO$_2$/epoxy composites improved by 46.6%, 37.81%, 42.09%, 86.86% and 46.56% compared to neat epoxy, respectively. The improvement was attributed to the synergistic effect among GO and SiO$_2$ and the strong interaction with the epoxy matrix, which might effectively promote the load transfer from the epoxy to the GO-SiO$_2$ sheets. It is believed that this work could provide an effective method for future material modification and a new way for the application of high-performance nanocomposites.

CRediT authorship contribution statement

Lichun Ma: Conceptualization, Methodology, Data curation, Writing – original draft. **Guojun Song:** Conceptualization, Methodology, Writing – review & editing. **XieChen Zhang:** Data curation, Formal analysis, Validation, Data curation. **Shaofeng Zhou:** Software, Data curation, Investigation. **Yaqing Liu:** Data curation, Resources, Funding acquisition, Investigation. **Luyan Zhang:** Project administration, Funding acquisition.

Declaration of Competing Interest

The authors declare that they have no known competing financial interests or personal relationships that could have appeared to influence
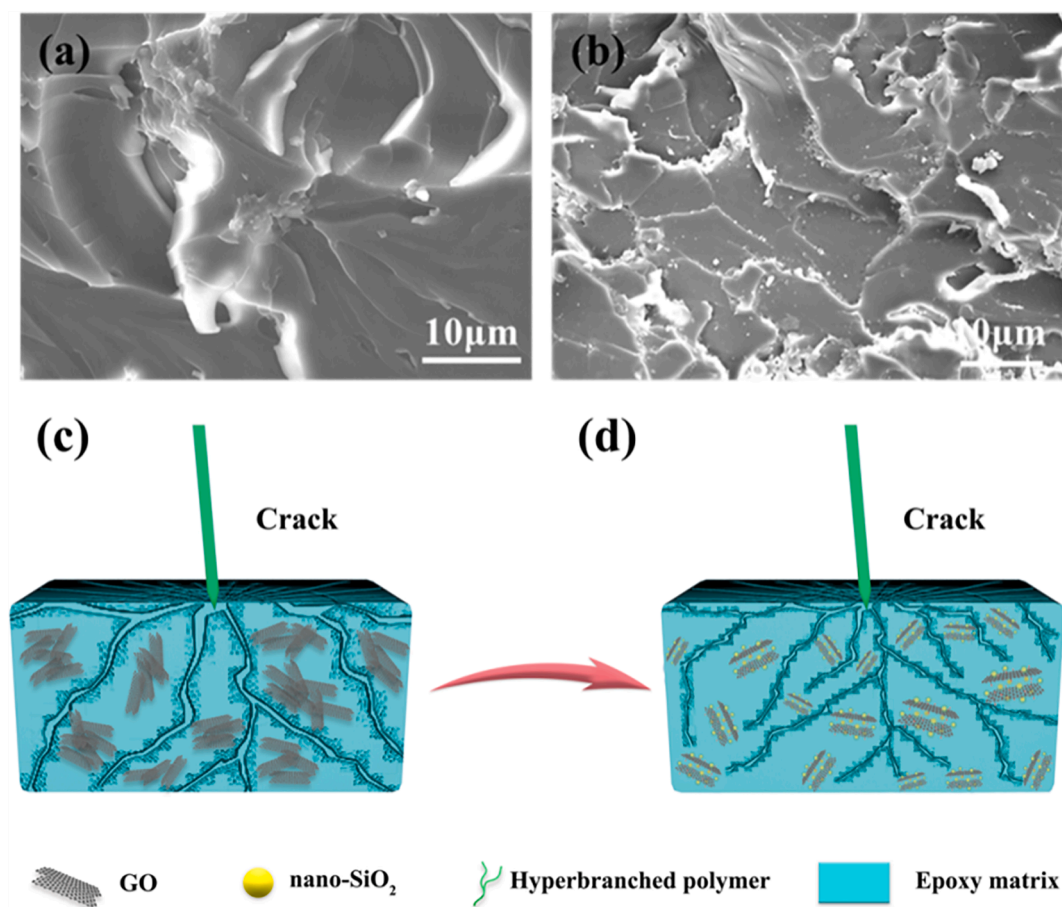

Fig. 8. SEM images of cross-sectional fracture surfaces and schematic diagram of failure mode: (a, c) GO; (b, d) GO-SiO$_2$.

the work reported in this paper.

Appendix A. Supplementary data

Supplementary data to this article can be found online at https://doi.org/10.1016/j.eurpolymj.2021.110677.

Reference

[1] L.J. Qu, Y.L. Sui, B.S. Xu, POSS-functionalized graphene oxide hybrids with improved dispersive and smoke-suppressive properties for epoxy flame-retardant application, Eur Polym J 122 (2020), 109383.

[2] C.Y. Lee, J.-H. Bae, T.-Y. Kim, S.-H. Chang, S.Y. Kim, Using silane-functionalized graphene oxides for enhancing the interfacial bonding strength of carbon/epoxy composites, Compos. Part A-Appl S. 75 (2015) 11–17.

[3] J. Zhang, Q. Kong, D.-Y. Wang, Simultaneously improving the fire safety and mechanical properties of epoxy resin with Fe-CNTs via large-scale preparation, J. Mater. Chem. A. 6 (15) (2018) 6376–6386.

[4] Y.T. Park, Y. Qian, C. Chan, T. Suh, M.G. Nejhad, C.W. Macosko, A. Stein, Epoxy toughening with low graphene loading, Adv. Funct. Mater. 25 (4) (2015) 575–585.

[5] M.Y. Wang, L.C. Ma, Y.D. Huang, G.J. Song, One-step generation of silica particles onto graphene oxide sheets for superior mechanical properties of epoxy composite and scale application, Compos. Commun. 22 (2020), 100514.

[6] X. Zhao, Y.e. Li, W. Chen, S. Li, Y. Zhao, S. Du, Improved fracture toughness of epoxy resin reinforced with polyamide 6/graphene oxide nanocomposites prepared via in situ polymerization, Compos. Sci. Technol. 171 (2019) 180–189.

[7] A.K. Geim, Graphene: status and prospects, Science. 324 (2009) 1530–1534.

[8] A.A. Balandin, S. Ghosh, W. Bao, I. Calizo, D. Teweldebrhan, F. Miao, C.N. Lau, Superior thermal conductivity of single-layer graphene, Nano. lett. 8 (3) (2008) 902–907.

[9] L.C. Ma, G.J. Song, Y.D. Huang, Reinforcing carbon fiber epoxy composites with triazine derivatives functionalized graphene oxide modified sizing agent, Compos. Part B-Eng. 176 (2019), 107078.

[10] W. Hou, Y.a. Gao, J. Wang, D.J. Blackwood, S. Teo, Nanodiamond decorated graphene oxide and the reinforcement to epoxy, Compos. Sci. Technol. 165 (2018) 9–17.

[11] V. Georgakilas, J.N. Tiwari, K.C. Kemp, J.A. Perman, A.B. Bourlinos, K.S. Kim, R. Zboril, Noncovalent functionalization of graphene and graphene oxide for energy materials, biosensing, catalytic, and biomedical applications, Chem. Rev. 116 (9) (2016) 5464–5519.

[12] C. Botas, P. Álvarez, P. Blanco, M. Granda, C. Blanco, R. Santamaría, L. J. Romasanta, R. Verdejo, M.A. López-Manchado, R. Menéndez, Graphene materials with different structures prepared from the same graphite by the Hummers and Brodie methods, Carbon. 65 (2013) 156–164.

[13] G.B. Huang, S.Q. Huo, X.D. Xu, W. Chen, Y.X. Jin, R.R. Li, P.G. Song, H. Wang, Realizing simultaneous improvements in mechanical strength, flame retardancy and smoke suppression of ABS nanocomposites from multifunctional graphene, Composites Part B 177 (2019), 107377.

[14] L.C. Ma, Y.Y. Zhu, P.F. Feng, G.J. Song, Y.D. Huang, H. Liu, Reinforcing carbon fiber epoxy composites with triazine derivatives functionalized graphene oxide modified sizing agent, Composites Part B 176 (2019), 107078.

[15] F. Fang, S.Y. Ran, Z.P. Fang, P.G. Song, H. Wang, Improved flame resistance and thermo-mechanical properties of epoxy resin nanocomposites from functionalized graphene oxide via self-assembly in water, Composites Part B 165 (2019) 406–416.

[16] M. Sahu, A.M. Raichur, Toughening of high performance tetrafunctional epoxy with poly (allyl amine) grafted graphene oxide, Compos. Part B-Eng. 168 (2019) 15–24.

[17] F. Liu, L. Wu, Y. Song, W. Xia, K. Guo, Effect of molecular chain length on the properties of amine-functionalized graphene oxide nanosheets/epoxy resins nanocomposites, RSC Adv. 5 (57) (2015) 45987–45995.

[18] S. Guo, L. Ma, G. Song, X. Li, P. Li, M. Wang, L. Shi, Z. Gu, Y. Huang, Covalent grafting of triazine derivatives onto graphene oxide for preparation of epoxy composites with improved interfacial and mechanical properties, J. Mater. Sci. 53 (24) (2018) 16318–16330.

[19] M.Y. Wang, L.C. Ma, G. Song, Chemical grafting of nano-SiO$_2$ onto graphene oxide via thiol-ene click chemistry and its effect on the interfacial and mechanical properties of GO/epoxy composites, Compos Sci Technol 182 (2019), 107751.

[20] M.Y. Wang, L.C. Ma, B.W. Li, W.J. Zhang, H. Zheng, G.S. Wu, Y.D. Huang, G. J. Song, One-step generation of silica particles onto graphene oxide sheets for superior mechanical properties of epoxy composite and scale application, Compos Commun 22 (2020), 100514.

[21] Z.D. Liu, B. Song, L. Wang, Significant improved interfacial properties of PBO fibers composites by in-situ constructing rigid dendritic polymers on fiber surface, Appl. Surf. Sci. 512 (2020), 145719.

[22] G.S. He, X. Li, L.F. Bai, L. Meng, Y. Dai, Y.S. Sun, C.C. Zeng, Z.J. Yang, G.C. Yang, Multilevel core-shell strategies for improving mechanical properties of energetic polymeric composites by the "grafting-from" route, Composites Part B 191 (2020), 107967.

[23] G.S. He, X. Li, Y.Q. Jiang, Y. Dai, R. Xu, C.C. Zeng, X.Q. Tu, Z.J. Yang, Bioinspired hierarchical interface design for improved mechanical and safety properties in energetic polymer composites, J Mater Sci 55 (2020) 15726–15740.

[24] L.C. Ma, G.S. Wu, Y.H. Wang, L.Y. Xu, G.J. Song, Hydroxyl-terminated triazine derivatives grafted graphene oxide for epoxy composites: Enhancement of interfacial and mechanical properties, Polymers. 11 (2019) 1866.

[25] S. Palraj, M. Selvaraj, K. Maruthan, G. Rajagopal, Corrosion and wear resistance behavior of nano-silica epoxy composite coatings, Prog Org Coat 81 (2015) 132–139.

[26] Y. Han, T. Wang, X. Gao, T. Li, Q. Zhang, Preparation of thermally reduced graphene oxide and the influence of its reduction temperature on the thermal, mechanical, flame retardant performances of PS nanocomposites, Compos Part A-Appl S 84 (2016) 336–343.

[27] Y. Ma, H. Di, Z. Yu, L. Liang, L. Lv, Y. Pan, Y. Zhang, D. Yin, Fabrication of silicadecorated graphene oxide nanohybrids and the properties of composite epoxy coatings research, Appl Surf Sci 360 (2016) 936–945.

[28] Z. Liu, H. Zhang, S. Song, Y. Zhang, Improving thermal conductivity of styrene-butadiene rubber composites by incorporating mesoporous silica@ solvothermal reduced graphene oxide hybrid nanosheets with low graphene content, Compos Sci Technol 150 (2017) 174–180.

[29] H. X, X.R. Li, P.Y. Li, G.J. Song, Enhancing mechanical performances of polystyrene composites via constructing cabon nanotube/graphene oxide aerogel and hot pressing, Compos Sci Technol, 195(2020)108191.

[30] Y.J. Wan, L.C. Tang, D. Yan, L. Zhao, Y.B. Li, L.B. Wu, J.X. Jiang, G.Q. Lai, Improved dispersion and interface in the graphene/epoxy composites via a facile surfactant-assisted process, Compos Sci Technol 82 (2013) 60–68.

[31] L.L. Cong, X.R. Li, L.C. Ma, Z. Peng, C. Yang, P. Han, G. Wang, G.J. Song, High-performance graphene oxide/carbon nanotubes aerogel-polystyrene composites: Preparation and mechanical properties, Meter Lett 214 (2018) 190–193.

[32] C.M. Damian, M.I. Necolau, I. Neblea, E. Vasile, H. Iovu, Synergistic effect of graphene oxide functionalized with SiO$_2$ nanostructures in the epoxy nanocomposites, Appl Sur Sci 507 (2020), 145046.

[33] S.Z. Haeri, B. Ramezanzadeh, M. Asghari, A novel fabrication of a high performance SiO$_2$-graphene oxide (GO) nanohybrids: Characterization of thermal properties of epoxy nanocomposites filled with SiO$_2$-GO nanohybrids, J Colloid Interf Sci 493 (2017) 111–122.

[34] J. Li, W. Zhu, S. Zhang, Q. Gao, J. Li, W. Zhang, Amine-terminated hyperbranched polyamide covalent functionalized graphene oxide-reinforced epoxy nanocomposites with enhanced toughness and mechanical properties, Polym Test 76 (2019) 232–244.

[35] X. Wang, N. Li, J. Wang, G. Li, X.G. Jian, Hyperbranched polyether epoxy grafted graphene oxide for benzoxazine composites: Enhancement of mechanical and thermal properties, Compos Sci Technol 155 (2018) 11–21.

[36] P. Xie, Y. Liu, M. Feng, M. Niu, C. Liu, N. Wu, K. Sui, R.R. Patil, D. Pan, Z. Guo, R. Fan, Hierarchically porous Co/C nanocomposites for ultralight high-performance microwave absorption, Adv Compos Hybrid Ma 4 (1) (2021) 173–185.

[37] P. Feng, L. Ma, G. Wu, X. Li, M. Zhao, L. Shi, M. Wang, X. Wang, G. Song, Establishment of multistage gradient modulus intermediate layer between fiber and matrix via designing double "rigid-flexible" structure to improve interfacial and mechanical properties of carbon fiber/resin composites, Compos Sci Technol 200 (2020) 108336, https://doi.org/10.1016/j.compscitech.2020.108336.

[38] L. Ma, Z. Bi, Y. Xue, W. Zhang, Q. Huang, L. Zhang, Y. Huang, Bacterial cellulose: an encouraging eco-friendly nano-candidatefor energy storage and energy conversion, J Mater Chem 8 (12) (2020) 5812–5842.